Available online at www.sciencedirect.com
SCIENCE DIRECT
Sensors and Actuators A 126 (2006) 277–286
SENSORS AND ACTUATORS A PHYSICAL
www.elsevier.com/locate/sna

Passive wireless strain monitoring of actual tire using capacitance–resistance change and multiple spectral features

Ryosuke Matsuzaki *, Akira Todoroki

Department of Mechanical Sciences and Engineering, Tokyo Institute of Technology, 2-12-1-I1-58 O-okayama, Meguro-ku, Tokyo 152-8552, Japan

Received 29 June 2005; accepted 18 October 2005
Available online 1 December 2005

Abstract

To improve reliability of automobile tires and anti-lock braking system (ABS), intelligent tires that measure strain of tires are increasingly demanded. The high stiffness of an embedded sensor like a strain gage, however, causes debonding of a sensor from tire rubber. In a previous study, the authors proposed a wireless strain monitoring method that adopts a rectangular tire specimen as a sensor with a tuning circuit. Compared to the tire specimen, an actual tire has a large hysteresis between the measured strain of the inner tire surface and the capacitance in a tire belt. The large hysteresis in the actual tire makes it difficult to measure a tire strain precisely. In the present study, to measure the strain precisely, multiple power spectrum features of the sensor output are used to estimate the strain with a statistical method. As the spectral features, a peak power spectrum and a sharpness of the resonance in addition to a tuning frequency are used for the estimating. As a result the experiments demonstrate that the method is effective for the passive wireless strain monitoring of actual radial tires.

Keywords: Wireless sensor; Strain monitoring; Tire; Tuning circuit; Power spectrum; Quality factor

1. Introduction

As a result of the recall of Firestone Co. tires in 2000, U.S. Transportation Recall Enhancement, Accountability and Documentation (TREAD) legislation has mandated the installation of Tire Pressure Monitoring Systems (TPMSs) [1–10]. A simple method for TPMS is based on indirect measurement using wheel speed sensors and electronic control unit (ECU) of anti-lock braking system (ABS) [1,2]. The indirect measurement, however, depends on the type of the tire and needs calibration, which causes low reliability. Direct measurement of TPMS has been developed using clamp-on-rim sensors by SmarTire System Inc. in Canada or valve-attached sensors by Schrader Electronics Ltd. in UK. Although these methods have high accuracy and reliability for the pressure monitoring, they need battery to activate the sensors. For a battery-less TPMS, Snyder [3] proposed piezoelectric reed included in a tire sensor unit. The wheel movements cause the piezoelectric reed to bend and generate electricity.

Advanced tire sensor system is under developing as "intelligent tire" which is equipped with a sensor to monitor strain, air pressure, temperature, etc., of a tire to improve automobile safely [11–23]. In Europe, a EU-project named APOLLO (2002–2005) [4] was started to develop intelligent tires. A tire strain monitoring system that has sensors transmitting the tire strain to ABS or electronic stabilization program (ESP) systems is demanded to enhance security of tires. Contrary to the indirect measurement of friction between a tire and a load surface based on the wheel slip [24,25], the direct monitoring of tire strain allows precise measurement of friction, and hence it increases the efficiency of ABS. As a direct method for tire strain monitoring, Pohl et al. [11] proposed surface acoustic wave sensors, and Palmer et al. [12] proposed optical fiber sensors to monitor strain of the tire. Intelligent tires also offer beneficial effects for the other advanced active safely systems such as traction control systems (TCSs) and vehicle stability assist (VSA), early detection of tire separation [13] and tire-burst prevention [14].

The key technology for the intelligent tire sensor is direct measurement, wireless data transmission, battery-less power supply and low stiffness sensor. The stiffness of the integrated or attached sensors is usually much higher than

* Corresponding author. Tel.: +81 3 5734 3178; fax: +81 3 5734 3178.
E-mail address: rmatsuza@ginza.mes.titech.ac.jp (R. Matsuzaki).

0924-4247/$ – see front matter © 2005 Elsevier B.V. All rights reserved.
doi:10.1016/j.sna.2005.10.029

that of tire rubber. The large difference in stiffness may disturb deformation and stress of tires; it may also cause the debonding of sensors and rubber over a long period use. The attached sensors are also easily damaged by fatigue of 10^6 cycles during tire lifetime or abrupt large deformation. A wireless monitoring is indispensable because a tire usually rotates.

In the previous study [15–20], we have demonstrated dynamic strain monitoring of tires using a change in capacitance of a tire itself. The proposed sensor module using tuning circuit is passive type and does not need any power supply [20]. In this method, the capacitance change between two adjacent steel wires in an actual tire belt is adopted as a strain sensor. Since the tire itself performs as a sensor, the sensor does not cause the debonding from the tire surface. The proposed system was applied to a tire specimen. The specimen is a rectangle belt part cut from a commercially available radial tire in size of 270 mm in length and 20 mm in width. The deformation of the steel wire in the specimen is limited in the in-plane direction. As a result, the output of the tuning frequency changes linearly to the applied tensile strain to the tire specimen. This linear change in the tuning frequency enables us to measure the applied strain precisely.

The structure of an actual tire is, however, three-dimensionally layered with a carcass, a belt and a tread. Moreover, in the actual tire, a compressive load is applied to a tire due to contacting a road surface. It causes a bending load to an actual tire surface unlike the tensile test using a tire specimen. Compared to the tire specimen, the actual tire has a large hysteresis between a strain of the inner tire surface measured by means of an attached strain gage and the capacitance in the tire belt. The hysteresis is caused by following reasons: the deformation paths in loading and unloading are different from each other due to the complexity of the actual tire structure; the viscoelastic belt in the actual tire deforms delaying against the deformation of an elastic strain gage, while the deformation of the thin tire specimen does not delay because it behaves like an elastic material due to the adhesion of a strain gage. The large hysteresis in the actual tire makes it difficult to measure a tire strain precisely because the each capacitance value corresponds to two different strain values.

Since the tire rubber is not pure dielectric material and acts also as an electrical resistor [21], it can be assumed as a capacitance–resistance parallel model. To measure a tire strain precisely, we utilize multiple kinds of variables: the electric resistance and the capacitance of an actual tire. The values of the multiple variables enable us to know whether the condition is loading or unloading, and it is possible to measure the strain precisely.

In the present paper, the effects of the deformation of the tire belt on the electric resistance and the capacitance are experimentally investigated. The tuning circuit is employed here to transmit the electric resistance and the capacitance data wirelessly to an external receiver. To measure the tire strain precisely and wirelessly, multiple spectral features of the sensor output instead of the electric resistance and the capacitance are used for estimating the strain with a statistical method. As the spectral features, a peak power spectrum and a sharpness of the resonance in addition to the tuning frequency are used for the estimating. The tuning frequency and the peak power spectrum reflect the capacitance and the electric resistance, respectively, the sharpness of the resonance reflects both the electric resistance and the capacitance. Although the resonance point features like the tuning frequency and the peak power spectrum are easily affected by an environmental noise, the sharpness of the resonance is not affected because it is measured using whole power spectrum shape. Using these multiple spectral features and a statistical method, the proposed sensor system is applied to a commercially available tire, and the applicability of the proposed sensor is examined.

2. Wireless strain monitoring system

2.1. Structure of tire belt

The passive wireless strain measurement system employs a tire itself as a sensor. Fig. 1 shows a typical radial tire's inner structure. Carcass fibers are perpendicular to the beads wire on radial tires as shown in Fig. 1. The carcass's function is to maintain the shape of the tire. Usually the carcass fiber is an organic fiber such as polyester. On the carcass fiber layer, steel wire layers are mounted similarly to cross-ply laminates of composite materials. These fibers are coated with rubber, and the tread rubber layer is mounted on the steel wire layers, as shown in Fig. 1. Tread deformation is transferred to the steel wire layers. This transferral implies that measurement of the steel wire layer strain indicates the tire tread deformation.

In the steel wire layer, the steel wire is a straight electrically conductive material; the rubber is a dielectric and electrically resistive material. Fig. 2 shows a couple of adjacent steel wires. In this figure, the steel wires are placed face-to-face; the dielectric rubber is inserted between the two steel wires. Electric voltage is charged between the steel wires. This structure thereby represents a parallel circuit of an electric resistor and a condenser. The adjacent steel wires are electrodes of these electric resistor and the condenser.

Let us consider the adjacent steel wires are given electric charges per unit length, q, $-q$, respectively. From Gauss' law, the electric field on the line through centers of the adjacent steel

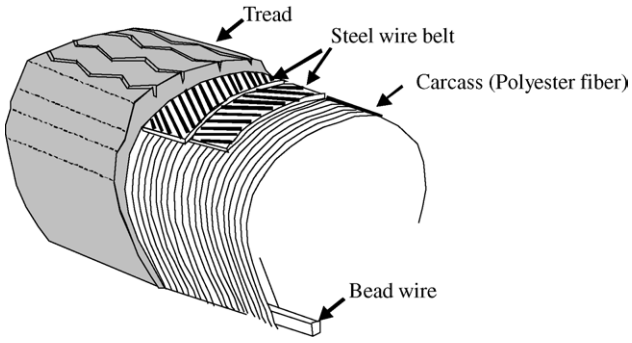

Fig. 1. Inner structure of a steel wire-reinforced radial tire.

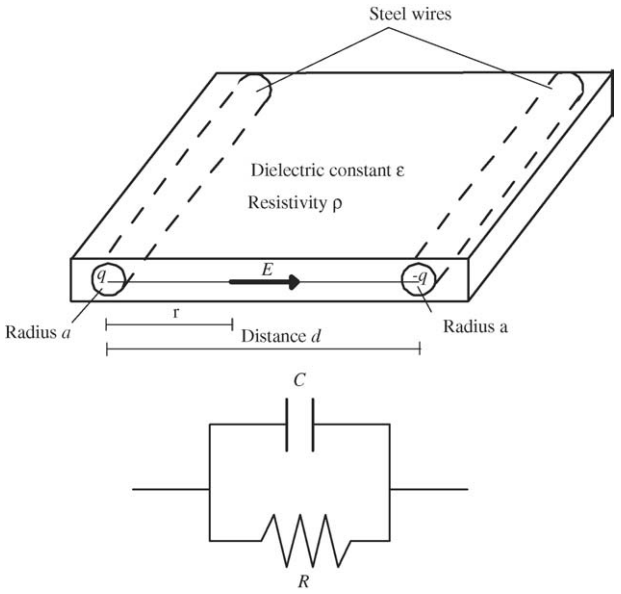

Fig. 2. Electric resistor–condenser parallel model of a steel wire belt in a radial tire.

wires, E, at distance, r, from a steel wire as shown in Fig. 2 is given as follows:

$$E_r = \frac{q}{2\pi\varepsilon r} + \frac{q}{2\pi\varepsilon(d-r)} \tag{1}$$

where ε is the dielectric constant of the tire rubber and d is the spacing between the adjacent steel wires.

Eq. (1) gives the difference in potential between adjacent steel wires, V, as follows:

$$V = -\int_{d-a}^{a} E_r \, \mathrm{d}r = \frac{q}{\pi\varepsilon} \ln\left(\frac{d-a}{a}\right) \tag{2}$$

where a is a radius of a steel wire in the tire.

Eq. (2) shows the electric capacitance of the condenser per unit length, C, as follows:

$$C = \frac{q}{V} = \frac{\pi\varepsilon}{\ln\frac{d-a}{a}} \tag{3}$$

Considering the tire rubber as an electric resistor, the electric resistance between electrodes is expressed as follows:

$$R = \rho\frac{d}{2al} \tag{4}$$

where ρ is resistivity of the rubber.

The spacing d is enlarged when the steel wire layer is elongated, implying that the capacitance is reduced from Eq. (3), and the electric resistance increases from Eq. (4). This indicates that the tire deformation alters the tire's electric resistance and the capacitance. The changes in the electric resistance and the capacitance of the tire belt enable us to know the applied strain of the actual tire.

2.2. Tuning frequency and peak power spectrum

The present study adopts a simplified passive tuning circuit for sending the change in the electric resistance and the capacitance of tires to an external receiver wirelessly. Fig. 3 shows a schematic image of the present passive wireless monitoring

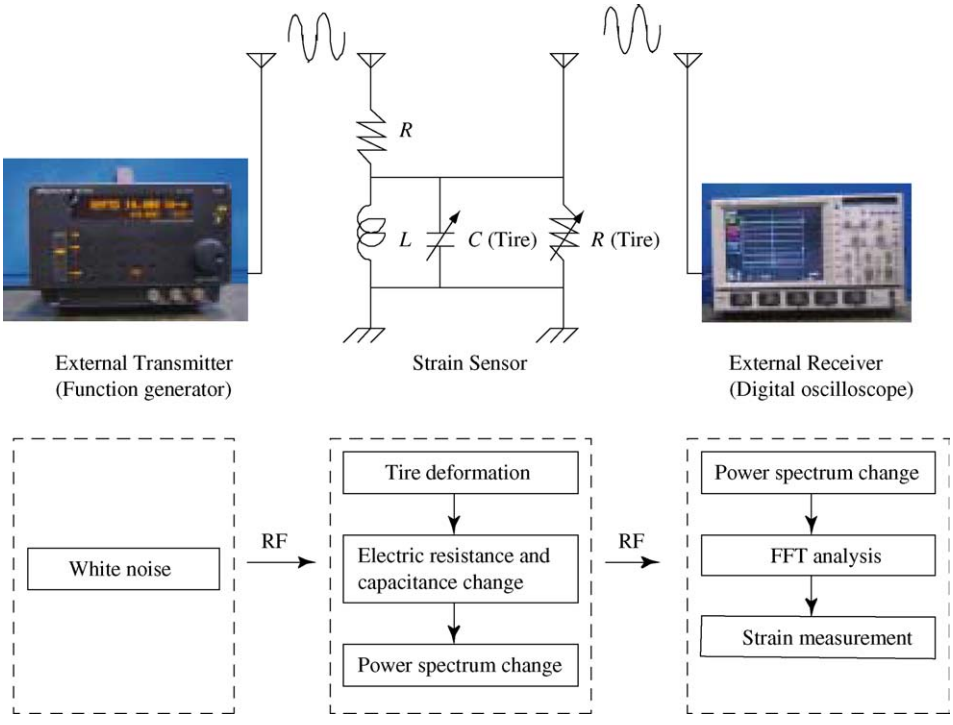

Fig. 3. Schematic image of the wireless passive strain measurement system.

system. Systems comprise an external transmitter, a strain sensor and an external receiver. The wireless strain measurement system uses four antennas, including one for the output of the external transmitter, two for the input and the output of the sensor module and one for the input of the external receiver. The antennas are wire type and 150 mm long. This monitoring system provides following advantages. First, the tire itself is adopted as a sensor. Thereby, this method avoids sensor debonding during a long period use and disturbance of the tire stress and deformation field. Second, the strain sensor system is a passive wireless type. Such a passive wireless sensor requires no batteries to activate the sensor circuit. This battery-less system achieves weight reduction and long-term stabilization.

The transmitter is employed here to emit radio waves of white noise. It is easily produced using a normal function generator. The transmitted white noise is picked up with the tuning circuit antenna. The tuning circuit comprises the inductance (L in henries) of a coil, the tire electric resistance (R in ohms) and the tire capacitance (C in farads). This is a pure LCR parallel resonator circuit The combined admittance of the resonant circuit, Y, is given as follows:

$$Y = \frac{1}{R} + \mathrm{j}\left(\omega C - \frac{1}{\omega L}\right) \tag{5}$$

where j is $\sqrt{-1}$ and ω is the radian frequency in hertz.

The right side of Eq. (5) ($\omega C - (1/\omega L)$) is set equal to zero to find the tuning frequency of strain sensor, f_t:

$$f_\mathrm{t} = \frac{\omega}{2\pi} = \frac{1}{2\pi\sqrt{LC}} \tag{6}$$

From Eq. (5), the admittance at the tuning frequency, Y_0, is given as follows:

$$Y_0 = \frac{1}{R} \tag{7}$$

The peak power spectrum at the tuning frequency, P_p, is given as follows:

$$P_\mathrm{p} = \frac{I^2}{Y_0} = I^2 R \tag{8}$$

where I is applied current to the LCR parallel circuit.

Eq. (6) shows that the increase in the capacitance C decreases the tuning frequency f_t, and Eq. (8) shows that increase in the electric resistance R increases the peak power spectrum P_p when the inductance L is fixed.

When the applied stress deforms the tire specimen, the change in the spacing between steel wires causes the change in the electric resistance and the capacitance of the tire belt. Consequently, deviation occurs from the tuning circuit resonance as the tuning frequency and the peak power spectrum. The tuned radio wave at the frequency f_t is picked up at the external receiver. The tuning frequency and the peak power spectrum of the received wave are calculated by means of fast Fourier transform (FFT). Eqs. (6) and (8) show that measurement of the tuning frequency and the peak power spectrum indicates the changes in the tire's electric capacitance and the resistance, respectively.

Since the antenna at the external receiver receives the signal from the sensor as well as the direct signal from the transmitter, electromagnetic shield is needed between the white noise area and sensor output area. The white noise area includes the output antenna of the external transmitter and the input antenna of the sensor module. The sensor output area includes the output antenna of the sensor module and the input antenna of the external receiver. In a practical use, the output antenna of the external transmitter and the input antenna of the sensor are placed inside of the tire, and the output antenna of the sensor and the input antenna of the external receiver are placed outside of the tire such as a outer surface of the wheel.

2.3. Quality factor

The sharpness of the resonance is widely expressed as quality factor Q. The quality factor is defined by the half power bandwidth (HBW) method otherwise known as the 3 dB method [26]. The half power points are points where the amplitude response is reduced by 0.707 of its peak value or at which the power drops to 3 dB level. The quality factor is expressed as follows:

$$Q = \frac{f_\mathrm{t}}{f_2 - f_1} \tag{9}$$

where f_1 and f_2 are frequencies when the voltage drop E is the half value of the E_0 at the tuning frequency. Since the voltage drop E is in inverse proportion to admittance Y, following equation is obtained:

$$\frac{|E|}{E_0} = \frac{Y_0}{|Y|} = \frac{1}{R\sqrt{\frac{1}{R^2} + \left(\omega C - \frac{1}{\omega L}\right)^2}} \tag{10}$$

Since the fraction E/E_0 is 1/2 when the frequency is equal to f_1 or f_2 the frequency f_1 and f_2 are the root of following equation:

$$\left(2\pi f C - \frac{1}{2\pi f L}\right) R = \pm 1 \tag{11}$$

Solving Eq. (11) for frequency f the frequency f_1 and f_2 are obtained as follows:

$$f_1 f_2 = \frac{1}{4\pi LCR}(\pm L + \sqrt{L^2 + 4LCR^2}) \tag{12}$$

From Eqs. (6), (9) and (12), the quality factor Q of the parallel LCR resonance is expressed as follows:

$$Q = R\sqrt{\frac{C}{L}} \tag{13}$$

Eq. (13) indicates that the quality factor Q is in proportion to the electric resistance and square root of the capacitance of the tire.

The strain measurement of the tire is conducted by using the changes in the electric resistance and the capacitance due to the deformation of the tire steel belt. The change in the tuning frequency corresponds to the change in the capacitance of the tire; the change in the peak power spectrum corresponds to the change in the electric resistance. Thus, monitoring the tuning frequency and peak power spectrum enables us to know the

electric resistance and the capacitance of the tire. To improve the accuracy of estimation, the quality factor is added to the measurement data because the quality factor is measured by using the whole spectrum figuration, and more stable than the tuning frequency or the peak power spectrum. The applied strain of the tire, y, is estimated using three measurement data, f_t, P_p and Q instead of C and R as follows:

$$y = g(C, R) = f(f_t, P_p, Q) \tag{14}$$

When multiple channels of N are demanded, the required number of sensors is N in this case, but only a single receiver is needed. To distinguish each output signal, each sensor has to use different initial tuning frequencies from each other: f_1, f_2, ..., f_N. The power spectrum of the sensor of the number i, P_i, has a peak at the initial tuning frequency f_i. The power spectrum P of the received signal with the external receiver is the sum of the power spectrum P_i of each sensor as follows:

$$P = \sum_{i=1}^{n} P_i(f) \tag{15}$$

Since the power spectrum, P, has N peaks at the each initial tuning frequency, f_i, measurement of the frequency change of each peak enables us to obtain the electrical resistance changes of the multi-channels when each peak of the initial frequency has enough spacing.

2.4. Response surface method

For an actual tire, it is very difficult to find the precise model how the electric resistance and the capacitance change due to the deformation of tire because of the complexity of the tire structure. The response surface methodology [27] is adopted as a solver for the prediction of the applied strain to the actual tire. The response surface is a widely adopted tool for quality engineering fields. The response surface methodology brings two advantages: the inverse problems can be approximately solved without consideration of modeling of functions, and the approximated response surface can be evaluated using statistical tools.

The tire strain is estimated from measured multiple spectral features such as the tuning frequency, the peak power spectrum and the quality factor using response surface method. The complicated three-dimensional deformation of tire be It is easily approximated statistically. For most of the response surfaces, the functions for the approximations are polynomials because of the simplicity.

For the cases of quadratic polynomials, the response surface is described as follows:

$$y = \beta_0 + \sum_{j=1}^{k} \beta_j x_j + \sum_{j=1}^{k} \beta_j x_j^2 + \sum_{i=1}^{k} \sum_{j>i}^{k} \beta_{ij} x_i x_j \tag{16}$$

where k is the number of variables. In this study, the tuning frequency, the peak power spectrum and the quality factor are the variables: x_1, x_2 and x_3. The response surface is expressed as follows:

$$y = \beta_0 + \beta_1 x_1 + \beta_2 x_2 + \beta_3 x_3 + \beta_4 x_1^2 + \beta_5 x_2^2 + \beta_6 x_3^2 + \beta_7 x_1 x_2 + \beta_8 x_2 x_3 + \beta_9 x_3 x_1 \tag{17}$$

Substituting as $x_4 = x_1^2$, $x_5 = x_2^2$, $x_6 = x_3^2$, $x_7 = x_1 x_2$, $x_8 = x_2 x_3$ and $x_9 = x_3 x_1$, Eq. (17) becomes a liner regression model as follows:

$$y = \beta_0 + \sum_{i=1}^{9} \beta_i x_i \tag{18}$$

In the case that the total number of experiments is n, the response surface can be expressed as follows using matrix expression:

$$\mathbf{Y} = \mathbf{X}\boldsymbol{\beta} + \boldsymbol{\varepsilon} \tag{19}$$

where $\mathbf{Y}$ is response vector, $\mathbf{X}$ the experimental coordinate, $\boldsymbol{\beta}$ the coefficient vector and $\boldsymbol{\varepsilon}$ is error vector.

The unbiased estimator, $\mathbf{b}$, of the coefficient vector $\boldsymbol{\beta}$ is obtained using a least square error method as follows:

$$\mathbf{b} = (\mathbf{X}^{\mathrm{T}}\mathbf{X})^{-1}\mathbf{X}^{\mathrm{T}}\mathbf{Y} \tag{20}$$

In order to judge the goodness of the approximation of the response surface, the adjusted coefficient of multiple-determination R^2_{adj} is used.

$$R^2_{\mathrm{adj}} = 1 - \frac{\mathrm{SS_E}/(n-k-1)}{S_{\mathrm{yy}}/(n-1)} \tag{21}$$

where $\mathrm{SS_E}$ is the square sum of errors and S_{yy} is the total sum of squares.

Each coefficient of the response surface can be tested by using t-statistic. When the absolute value of the t-statistics is smaller than the threshold value of t-distribution ($t_{0.025, n-k-1}$), the coefficient is eliminated from the response surface as a non-significant coefficient to obtain higher R^2_{adj}.

3. Experimental procedures

3.1. Measurement of electric resistance and capacitance

The shoulder part of the tire tread is cut off to measure the electric resistance and the capacitance between the electrodes in the tire belt as shown in Fig. 4. The lead wire is soldered to the steel wire of the tire belt and used as electrodes for measurement of the electric resistance and the capacitance. The capacitance between two adjacent steel wires is about 30 pF. This capacitance value is too small to use as a capacitor in the circuit because it is easily affected by the stray capacitance in the sensor circuit or between the electric elements. Inter-digital electrodes as shown in Fig. 4, therefore, have been developed as the measurement electrodes to increase the change in the capacitance [19]. A conventional strain gage for rubber is attached to the inner surface of the tire for measurement of the tire strain. The electric resistance and the capacitance are measured by using LCR meter produced by HIOKI E.E. Corp., at measuring frequency

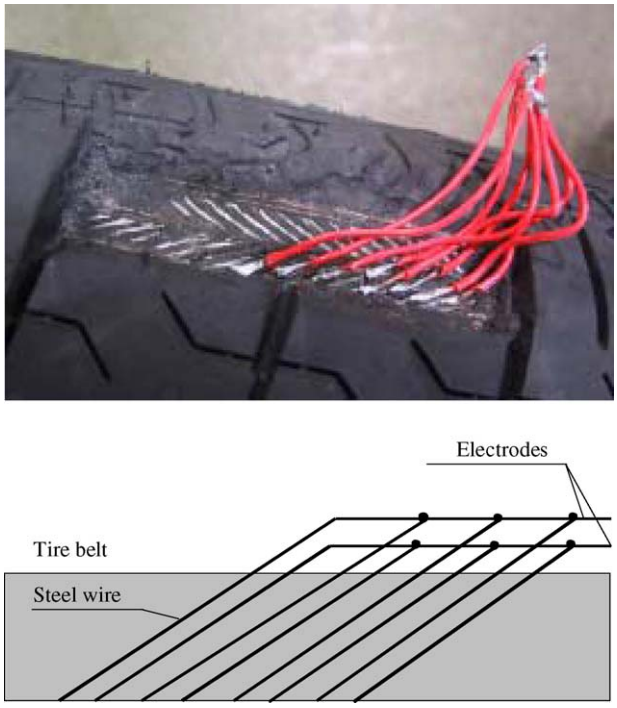

Fig. 4. Alignment of inter-digital electrodes of the tire belt.

of 100 kHz. Appling strain to the tire is performed using a tensile testing machine produced by SHIMAZU Corp. at crosshead speed of 2 mm/min.

3.2. Tuning frequency, peak power spectrum and quality factor

The sensor module is produced using the coil inductance of 100 μH as a sensor coil L. The output wave transmitted from a sensor module is picked up at the antenna of an external receiver wirelessly. The received wave is analyzed using a digital oscilloscope produced by LeCroy Ltd. Co.

The quality factor of the power spectrum is obtained using the frequency f_1 and f_2 at HBW as shown in Eq. (9). The problem in the used of the 3 dB method lies in the basic procedure to find the half power points. The obtained power spectrum is discrete instead of a continuous function, and not necessarily including the tuning frequency or the 3 dB bandwidth. Since this reduces the accuracy of measurement of the tuning frequency, the peak power spectrum or the quality factor, they have to be determined from the measurements by applying digital algorithms. In this study, the non-linear fitting to a Lorentzian curve is applied to estimate the spectral features precisely and robustly [28–30]. The Lorentzian function used as approximation function is expressed as follows:

$$P(f) = \frac{1}{\pi} \frac{\frac{1}{2}\Gamma}{(f-\mu)^2 + \left(\frac{1}{2}\Gamma\right)^2} \tag{22}$$

where Γ is full width at half maximum (FWHM) and μ is the frequency at mean power spectrum. Since these Γ and μ are the constants which have to be adjusted in order to agree with the experimental data, high calculation cost is required.

The quadratic polynomial approximation is possible using inverse of Lorentzian function as follows:

$$\frac{1}{P(f)} = \pi \frac{(f-\mu)^2 + \left(\frac{1}{2}\Gamma\right)^2}{\frac{1}{2}\Gamma} = k_0 f^2 + k_1 f + k_2 \tag{23}$$

where k_0, k_1 and k_2 are the coefficients which are easily obtained using least square method without high calculation cost.

From Eq. (23), the tuning frequency f_t, the peak power spectrum P_p and the quality factor Q are calculated as follows:

$$f_t = -\frac{k_1}{2k_2} \tag{24}$$

$$P_p = k_2 - \frac{k_1^2}{4k_0} \tag{25}$$

$$Q = \frac{-k_1}{4\sqrt{k_0 k_2 - \frac{1}{4}k_1^2}} \tag{26}$$

4. Experimental results and discussion

4.1. Electric resistance and capacitance

Fig. 5 shows the frequency response of the capacitance and the phase angle of an actual radial tire under no loading condition. The phase angle is between 0° and −90° under 1 MHz. This indicates that the belt in the actual tire can be assumed as a parallel circuit model of an electric resistor and a capacitor.

Fig. 6 shows the measured strain in the radial and longitudinal direction to the tire rotation due to the applied compressive loads when the sensor part is located at the road surface as shown in Fig. 7. The abscissa is crosshead displacement and ordinate is the measured strain by means of the attached strain gage. The strain in the longitudinal direction of the inner surface of the tire increases, and that in the transverse direction decreases with the increased compressive displacement.

Fig. 8 shows the changes in the electric resistance and the capacitance due to the applied strain using inter-digital

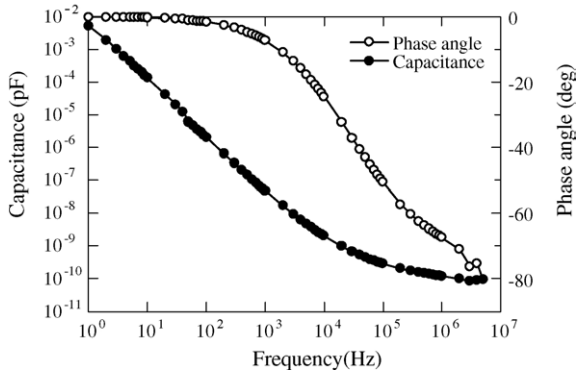

Fig. 5. Frequency response of the phase angle and the capacitance of a radial tire.

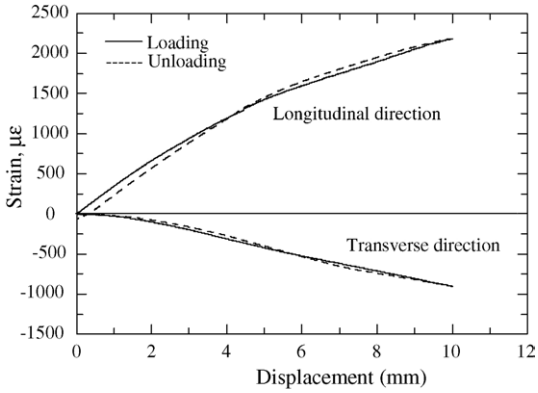

Fig. 6. Measured longitudinal strain and transverse strain vs. displacement due to loading and unloading.

electrodes on the tire belt. The abscissa is the measured strain in the longitudinal direction and the ordinate is the measured electric resistance and the capacitance. The electric resistance increases and the capacitance decrease with the increase of the applied strain. This is because that the inner surface at the contact point to the road surface is subjected to the tensile strain, which increases the spacing between steel wires. There is a large hysteresis of the measured electric resistance and the capacitance during loading and unloading, which makes it difficult to predict the strain precisely using only one variable of the electric resistance or the capacitance. Since the change in the capacitance is large enough, 600 pF, using the inter-digital electrodes, the effect of few stray capacitance is negligible.

4.2. Tuning frequency, peak power spectrum and quality factor

Fig. 9 shows the calculated tuning frequency, the peak power spectrum and the quality factor obtained from Eqs. (6), (8) and (13) using the experimental results of the changes in the electric

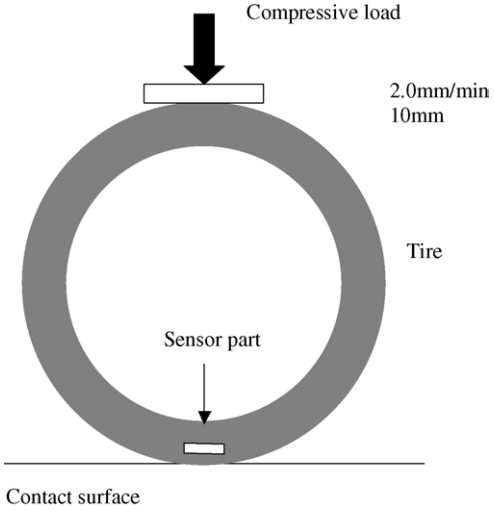

Fig. 7. Experimental setup for tire compression test.

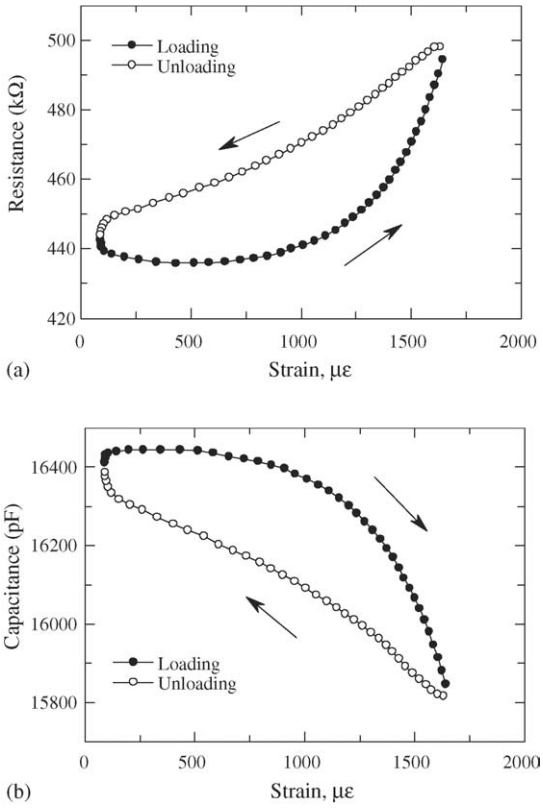

Fig. 8. Measured relationship between electric resistance, capacitance and strain using inter-digital electrodes: (a) electric resistance and (b) capacitance.

resistance and the capacitance as shown in Fig. 8(a and b). The abscissa is tire strain in the longitudinal direction, and the ordinate is the change ratio in the spectral features, $\Delta f/f_0$, $\Delta P_p/P_{p0}$ and $\Delta Q/Q_0$. The tuning frequency, the peak power spectrum and the quality factor increase with the increase of the applied strain as shown in Fig. 9. The figuration of power spectrum, therefore, changes with the applied strain as shown in Fig. 10: the mean frequency and maximum power spectrum increases and the spectral peak becomes sharper.

Fig. 11 shows the power spectrum of output fro ma sensor module using the tire belt as a sensor. The abscissa is the frequency and the ordinate is power spectrum. In the actual monitoring, the spectrum is swept from 450 to 625 kHz, and

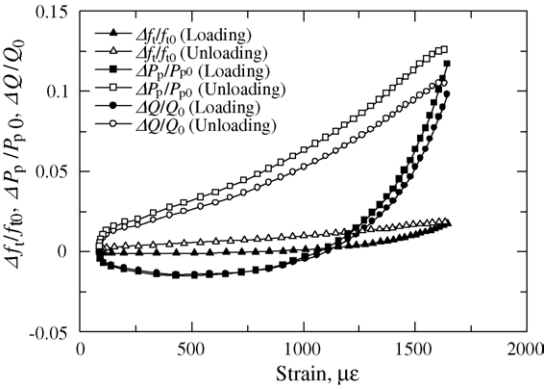

Fig. 9. Calculated $\Delta f_t/f_{t0}$, $\Delta P_p/P_{p0}$ and $\Delta Q/Q_0$ from Eqs. (6), (8) and (13).

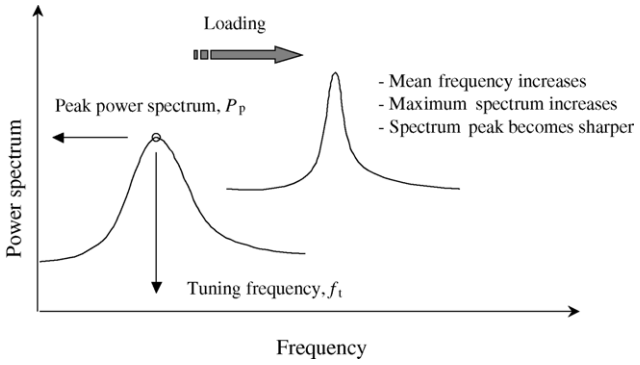

Fig. 10. The change in the power spectrum figuration due to loading.

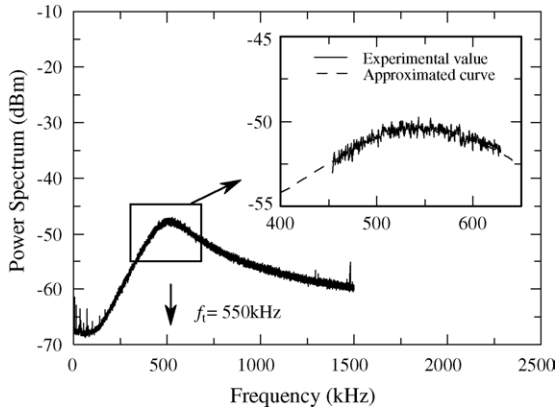

Fig. 11. Measured power spectrum of wirelessly received signal at external receiver.

the tuning frequency, the peak power spectrum and the quality factor are obtained from the power spectrum using Lorentzian curve fitting in Eq. (23) as shown in Fig. 11.

Figs. 12–14 show the wirelessly measured tuning frequency, the peak power spectrum and the quality factor due to the loading and unloading tests using an actual tire. The abscissa is measured strain and the ordinate is the change ratio in the spectral features, $\Delta f/f_0$, $\Delta P_p/P_{p0}$ and $\Delta Q/Q_0$. The tuning frequency decreases until the strain of 1000 μ and increases after 1000 μ. Since the tuning frequency does not change linearly to the applied strain, it is difficult to estimate the applied strain using only tuning frequency data. The peak power spectrum and the quality factor change monotone increasing. Figs. 12–14 agree with the calculated results as shown in Fig. 9. These results confirm that the changes in the tuning frequency, the peak power spectrum and the quality factor are caused by the changes in the electric resistance and the capacitance of a tire.

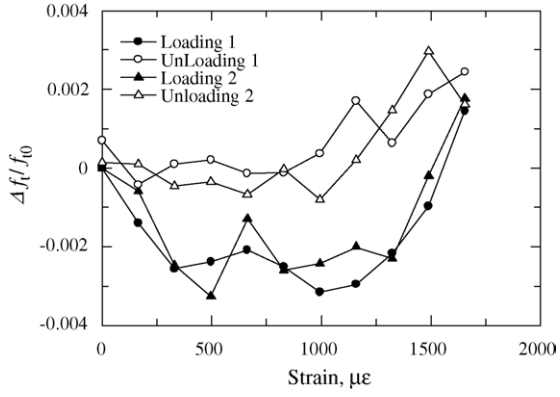

Fig. 12. Measured relationship between the change in the tuning frequency and the strain due to loading and unloading.

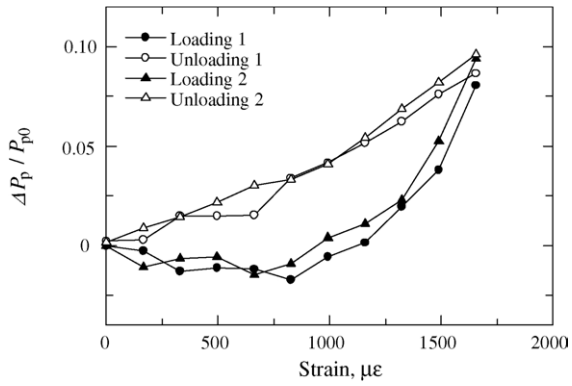

Fig. 13. Measured relationship between the change in the peak power spectrum and strain due to loading and unloading.

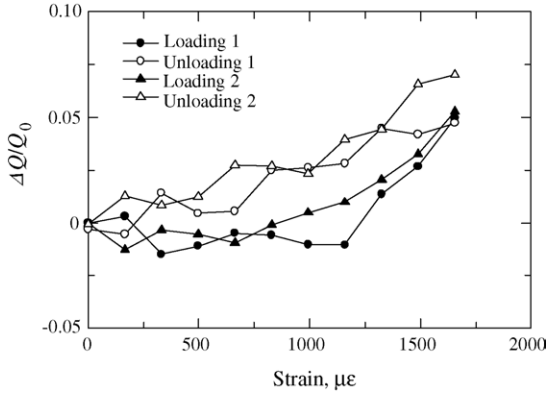

Fig. 14. Measured relationship between the change in the quality factor of resonance and strain due to loading and unloading.

Using the relationship between the spectral features and the applied strain, multiple regress function is obtained using response surface method. High accurate estimation is possible using three variables over the large strain range. Fig. 15 shows

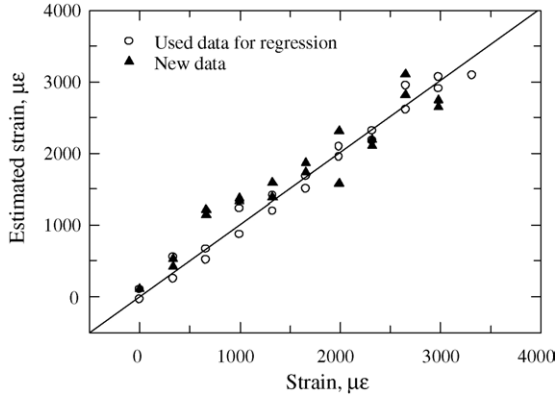

Fig. 15. Estimated strain and measured strain of tire.

Table 1
Comparison of R^2_{adj} using different parameter

	Loading	Unloading	Loading and unloading
f_t	−0.043	0.502	0.292
Q	0.781	0.927	0.708
P_p	0.791	0.909	0.806
f_t and Q	0.955	0.961	0.930
f_t and P_p	0.977	0.982	0.919
Q and P_p	0.791	0.981	0.730
f_t, Q and P_p	0.996	0.998	0.974

the estimation results substituting the tuning frequency, the peak power spectrum and the quality factor to the multiple regression model. The abscissa is the measured strain by means of a strain gage, and the ordinate is the estimated strain using response surface method. In this figure, the open circle symbols indicate experimental data used for making the regression model, and the solid triangle symbols show new experimental data. Since the R^2_{adj} is 0.974, the accuracy of the regression is high. The new experimental data are among the error band of 500 μ strain. Since the strain of the tire neither be measured nor obtained in the commercially available automobile, this estimation accuracy is enough useful for improving the automobile control. Table 1 shows the accuracy of estimation using the other variable sets as the response surface. The column shows the R^2_{adj} that response surface is made from only loading data, only unloading data or both loading and unloading data. From Table 1, the highest accurate estimation is obtained using three variables of f_t, P_p and Q.

5. Concluding remarks

The wireless strain measuring method is proposed using the electric resistance and the capacitance model of a tire belt The sensing system uses the changes in the tuning frequency, the peak power spectrum and the quality factor, and response surface method is used for the estimation of the applied tire strain.

(1) The electric resistance decreases and the capacitance increase with the applied strain to an actual radial tire.
(2) The tuning frequency, the peak power spectrum and the quality factor increase with the applied strain. The tuning frequency corresponds the capacitance, and the peak power spectrum corresponds the electric resistance.
(3) Using the spectrum features of the tuning frequency, the peak power spectrum and the quality factor, the tire strain is estimated accurately using response surface method.

Acknowledgment

Financial support form Bridgestone Corp. in Japan is acknowledged.

References

[1] N. Persson, S. Ahlqvist, U. Forssell, F. Gustafsson, Low tire pressure warning system using sensor fusion, SAE Conf. Proc. (1991) 77–79.
[2] F. Gustafsson, M. Drevo, U. Forsell, M. Lofgre, N. Persson, H. Quicklund, Virtual sensors of tire pressure and road friction, SAE technical papers, 2001, 2001-01-0796.
[3] D.S. Snyder, Piezoelectric reed power supply for use in abnormal tire condition warning systems, US-Patent 4,510,484, April 9, 1985.
[4] APOLLO Intelligent Tyre for Accident-Free Traffic, IST-2001-34372.
[5] K. Mnif, A smart tire pressure monitoring system, Sensors 12 (11) (2001) 40–46.
[6] T. Umeno, T.K. Asano, H. Ohashi, M. Yonetani, T. Naitou, T. Taguchi, Observer based estimation of parameter variations and its application to tyre pressure diagnosis, Control Eng. Pract. 9 (2001) 639–645.
[7] T. Yamagiwa, M. Orita, T. Harada, Development of a tire pressure monitoring system for motorcycles, JSAE Rev. 24 (4) (2003) 495–496.
[8] J.D. Cullen, N. Arvanitis, J. Cucas, A.I. Al-Shamma'a, In-filed trials of a tyre pressure monitoring system based on segmented capacitance rings, Measurement 32 (3) (2002) 181–192.
[9] C. Halfmann, M. Ayoubi, H. Holzmann, Supervision of vehicles' tyre pressures by measurement of body accelerations, Control Eng. Pract. 5 (8) (1997) 1151–1159.
[10] J. Siddons, A. Derbyshire, Tyre pressure measurement using smart low power microsystem, Sensor Rev. 17 (2) (1997) 126–130.
[11] A. Pohl, S. Reinhard, R. Leonhard, The "intelligent tire" utilizing passive SAW sensors—measurement of tire friction, IEEE Trans. Instrum. Meas. 48 (6) (1999) 1041–1046.
[12] M.E. Palmer, C.C. Boyd, J. McManus, S. Meller, Wireless smart-tires for road friction measurement and self state determination, in: 43rd AIAA/ASME/ASCE/AHS/ASC Structures, Structural Dynamics, and Materials Conference, AIAA, 2002, AIAA 2002-1548.
[13] A. Gavine, Common sense? The latest in vehicle safety comes courtesy of continental with its potentially life-saving tread deformation sensor, Tire Technol. Int. (2001) 32–33.
[14] S. Patwardhan, H.S. Tan, M. Tomizuka, Experimental results of a tire-burst controller for AHS, Control Eng. Pract. 5 (11) (1997) 1615–1622.
[15] A. Todoroki, S. Myatani, Y. Shimamura, Wireless strain monitoring using electrical capacitance change of tire: part I—with oscillating circuit, Smart Mater. Struct. 12 (2003) 403–409.
[16] A. Todoroki, S. Miyatani, Y. Shimamura, Wireless strain monitoring using electrical capacitance change of tire: part II—passive, Smart Mater. Struct. 12 (2003) 410–416.
[17] R. Matsuzaki, A. Todoroki, Passive wireless strain monitoring of tyres using capacitance and tuning frequency changes, Smart Mater. Struct. 14 (2005) 561–568.
[18] R. Matsuzaki, A. Todoroki, Wireless strain monitoring of tires using electric capacitance changes with an oscillating circuit, Sens. Actuators A 119 (2005) 323–331.
[19] R. Matsuzaki, A. Todoroki, H. Kobayashi, Y. Shimamura, Passive wireless strain monitoring of a tire using capacitance and electromagnetic induction change, Adv. Compos. Mater. 14 (2) (2005) 147–164.
[20] R. Matsuzaki, A. Todoroki, Passive wireless strain monitoring of tyres using capacitance and tuning frequency changes, Smart Mater. Struct. 14 (2005) 561–568.
[21] M. Srgio, N. Manaresi, M. Tartagni, R. Guerrieri, R. Canegallo, On road tire deformation measurement system using capacitive–resistive sensor, in: Proceedings of Second IEEE International Conference on Sensors: IEEE Sensors 2003, Toronto, Ont., Canada, October 22–24, 2003, pp. 1059–1063.
[22] M. Brandt, V. Bachmann, A. Vogt, M. Fach, K. Mayer, B. Breuer, H.L. Hartnagel, Highly sensitive AlGaAs/GaAs position sensors for measurement of lyre tread deformation, Electron. Lett. 34 (8) (1998) 760–762.
[23] O. Yilmazoglu, M. Brandt, J. Sigmund, E. Gene, H.L. Hartnagel, Integrated InAs/GaSb 3D magnetic field sensors for "the intelligent tire", Sens. Actuators A 94 (2001) 59–63.
[24] J. Yi, R. Horowitz, Adaptive emergency braking control with underestimation of friction coefficient, IEEE Trans. Control Syst. Technol. 10 (3) (2002) 381–392.
[25] F. Gustafsson, Slip-based tire-road friction estimation, Automatica 33 (6) (1997) 1087–1099.

[26] V.J. Logeeswaran, F.E.H. Tay, M.L. Chan, F.S. Chau, Y.C. Liang, First harmonic (2f) characterisation of resonant frequency and Q-factor of micromechanical transducers, Analog Integr. Circuits Signal Process. 37 (2003) 14–33.
[27] R.H. Myers, D.C. Montgomery, Response Surface Methodology: Process and Product Optimization Using Designed Experiments, John Wiley & Sons. Inc., 1995.
[28] R. Knochel, F. Daschner, W. Taute, Resonant microwave sensors of instantaneous determination of moisture in foodstuffs, Food Control 12 (2001) 447–458.
[29] R. Knochel, Technology and signal processing of dielectrometric microwave sensors for industrial applications, Sensors Update 7 (2000) 65–105.
[30] J. Molla, A. Ibarra, J. Margineda, J.M. Zamarro, A. Hernandez, Dielectric property measurement system at cryogenic temperatures and microwave frequencies, IEEE Trans. Instrum. Meas. 42 (1993) 817–821.

Biographies

Ryosuke Matsuzaki was born in Kanagawa, Japan, in 1980. He received his B Eng and M Eng in 2003 and 2004, respectively, in mechanical sciences and engineering form Tokyo Institute of Technology, Tokyo, Japan. He has been working as a graduate student of Tokyo Institute of Technology. His research interests include structural health monitoring, intelligent tires and composite materials. Ryosuke Matsuzaki is a member of The Japan Society of Mechanical Engineers, The Society of Materials Science, Japan, and The Japan Society of Composite Material.

Akira Todoroki was born in Japan in 1961. He received B Eng, M Eng and Dr Eng degrees in 1984, 1988 and 1991, respectively, all in mechanical sciences and engineering from Tokyo Institute of Technology, Tokyo, Japan. From 1986 to 1988, he was employed as researcher of Mitsubishi Heavy Industries, Nagoya Aircraft Works, from 1988 to 1944 as a research associate of Tokyo Institute of Technology and from 1995 to 1996 as a visiting researcher of the University of Florida. Since 1994, he has been serving as an associate professor of Tokyo Institute of Technology. His research interests include optimization of composite structures and smart composite structures. He has authored over 80 scientific papers and a portfolio of 8 patents. Prof. Todoroki has received two awards from The Japan Society of Mechanical Engineers in 1984 and 1989, two awards from The Society of Materials Science, Japan, in 2000 and 2005 and one award from The Japan Society for Composite Materials in 2000.